

1
2
3
4
5
6
7
8
9
10
11
12
13
14
15
16
17
18
19
20
21
22
23
24

Finite Element Modelling of the Foot for Clinical Application: a Systematic Review

Sara Behforootan, Panagiotis Chatzistergos*, Roozbeh Naemi, Nachiappan Chockalingam

Faculty of Health Sciences, Staffordshire University, Stoke-on-Trent, United Kingdom

*Corresponding Author

Panagiotis Chatzistergos

Faculty of Health Sciences

Staffordshire University

Leek Road

Stoke on Trent ST4 2DF

Email: Panagiotis.chatzistergos@staffs.ac.uk

25 Abstract:

26 Over the last two decades finite element modelling has been widely used to give new insight
27 on foot and footwear biomechanics. However its actual contribution for the improvement of
28 the therapeutic outcome of different pathological conditions of the foot, such as the
29 diabetic foot, remains relatively limited. This is mainly because finite element modelling is
30 only been used within the research domain. Clinically applicable finite element modelling
31 can open the way for novel diagnostic techniques and novel methods for treatment
32 planning/optimisation which would significantly enhance clinical practice.

33

34 In this context this review aims to provide an overview of modelling techniques in the field
35 of foot and footwear biomechanics and to investigate their applicability in a clinical setting.

36

37 Even though no integrated modelling system exists that could be directly used in the clinic
38 and considerable progress is still required, current literature includes a comprehensive
39 toolbox for future work towards clinically applicable finite element modelling. The key
40 challenges include collecting the information that is needed for geometry design, the
41 assignment of material properties and loading on a patient-specific basis and in a cost-
42 effective and non-invasive way. The ultimate challenge for the implementation of any
43 computational system into clinical practice is to ensure that it can produce reliable results
44 for any person that belongs in the population for which it was developed. Consequently this
45 highlights the need for thorough and extensive validation of each individual step of the
46 modelling process as well as for the overall validation of the final integrated system.

47

48

49 1. Introduction:

50 The ability to assess in vivo stresses that are developed inside the human foot during
51 clinically relevant scenarios would significantly enhance our understanding on foot
52 biomechanics and foot related pathologies. In the case of the diabetic foot, in particular, the
53 ability to calculate internal stresses could shed new light on the phenomena that lead to
54 ulceration and enable the optimisation of offloading strategies on a patient specific basis.

55

56 Despite this, there is no experimental method for the non-invasive assessment of internal
57 soft tissue stress. Moreover, the complex geometry and nonlinear mechanical behaviour of
58 the foot render any analytical solution practically impossible without significant
59 simplifications in terms of morphology and function [1].

60

61 Finite element (FE) is a powerful numerical method which can be utilised to solve problems
62 with complicated geometry, material properties and loading. Therefore it is no surprise that
63 current literature is rich in elaborate FE analyses on foot and footwear biomechanics. FE
64 analyses have already given new insights in the phenomena associated with ulceration of
65 the diabetic foot [2–9] and the offloading capabilities of diabetic footwear [4,6,10].
66 However, the actual contribution of FE analyses for the improvement of the therapeutic
67 outcome of the diabetic foot is relatively limited [11]. This is mainly because FE modelling
68 cannot be utilised outside the research domain to enhance and inform the everyday clinical
69 management of the diabetic foot, or other foot related pathological conditions [11].

70

71 One of the main challenges for the implementation of FE modelling in everyday clinical
72 practice is the development of reliable and affordable techniques for the subject specific

73 modelling of the foot. Although the ability to use any modelling technique in the clinic is
74 mainly determined by its ease of use, its non-invasive nature and low cost, the potential to
75 actually enhance clinical practice is determined to a great extent by the accuracy and
76 relevance of the information it can provide. Therefore, the main purpose of this review is to
77 provide an overview of different modelling approaches and simulation techniques that have
78 been used in the field of foot and footwear biomechanics and to investigate their
79 applicability in a clinical setting and where possible also to comment on their accuracy.

80

81

82 2. Method:

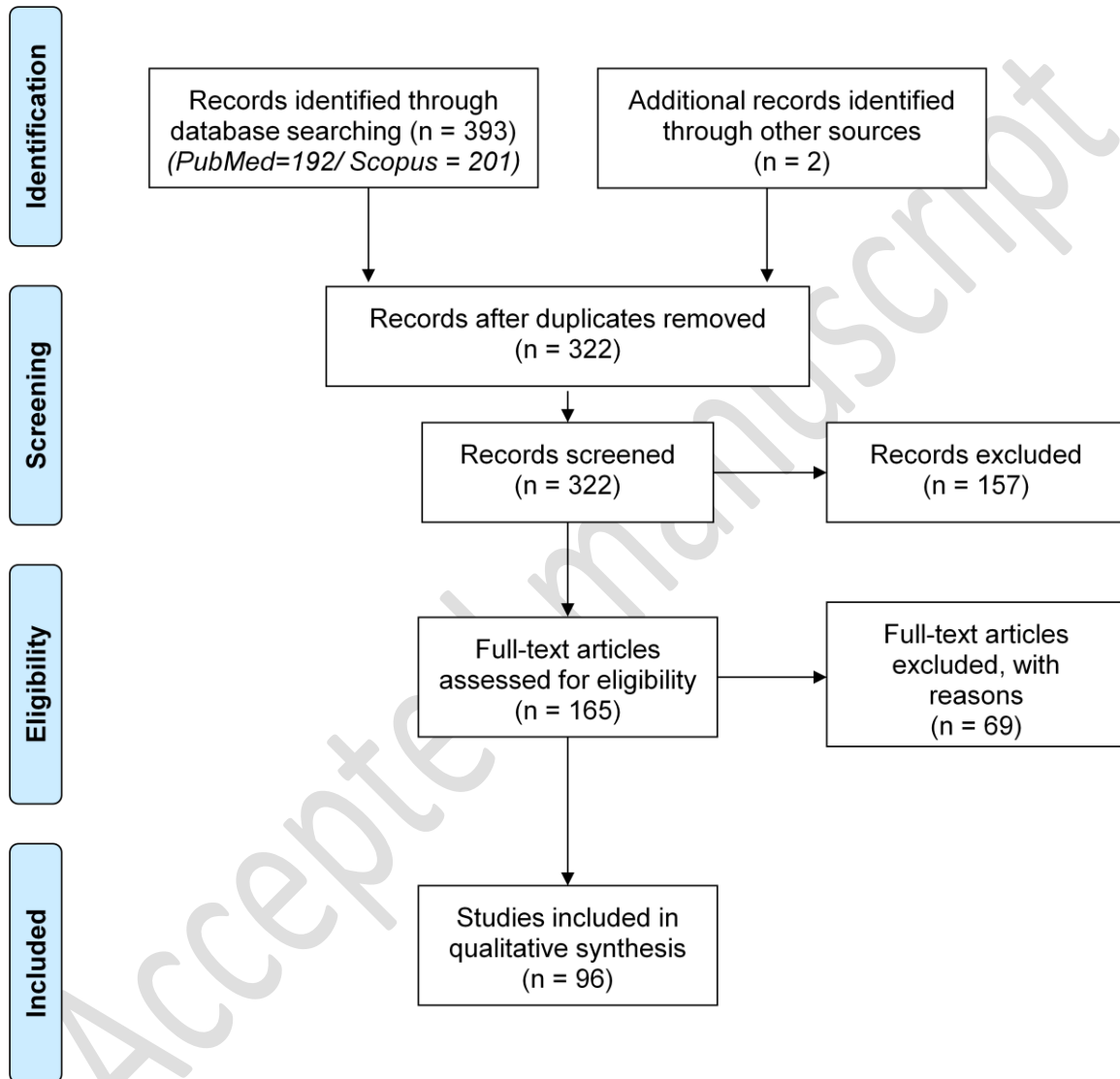
83 Relevant databases (Pubmed and Scopus) were searched using the keywords: (finite
84 element [Title/Abstract]) AND (foot [Title/Abstract] OR shoe [Title/Abstract] OR plantar
85 [Title/Abstract]) on 4th September 2015. The search was limited to studies with full texts
86 published in English but there was no limitation in terms of publication date.

87

88 This review considered original papers on FE analysis of both the entire foot and parts of
89 foot. In addition, FE analyses of footwear and insoles were also included. Analyses that were
90 not focused on the entire foot or parts of the foot but on musculoskeletal structures
91 proximal to the talus or the ankle joint were excluded. This means that studies on ankle,
92 knee or hip prostheses/orthoses as well as studies on fracture and fracture fixation of the
93 tibia and femur were all excluded. The papers which modelled foot with amputation were
94 also excluded. After removing the duplicates, the abstracts of 322 articles were screened
95 and 165 articles that met the criteria for inclusion based on abstract were selected. Full text
96 of all remaining articles were then assessed against the eligibility criteria leading to the

97 selection of 96 articles which met the inclusion criteria (Fig. 1). Selected papers were
98 analysed in terms of the methods used for: a) geometry design, b) the assignment of
99 material properties, c) the definition of boundary conditions and loading and d) validation.

100



101

102

103 Figure 1: Review flow chart (Prisma 2009).

104

105

106

107 These papers covered a wide range of applications in the broader area of foot biomechanics
108 and used a variety of different simulation strategies. More specifically 79% of reviewed
109 papers simulated the healthy foot and the remaining 21% the pathologic foot. Thirty three
110 percent (33%) in total were focused on the interaction between foot and footwear and 13%
111 were related to the diabetic foot. Detailed information about every study that was included
112 in this review can be found in supplementary material (S1 Table).

113

114

115 3. Results:

116 The methods that were used in these studies for designing the geometry, assigning the
117 material properties, defining loading and for validation are presented below. In each case
118 specific methods and their applicability in the clinical setting will be discussed after a brief
119 overview of the range of methods used.

120

121 3.1 FE model design

122 Two main methodological approaches were found for geometric design: The use of realistic
123 representations of foot geometry (89% of reviewed papers) or the use of idealised geometry
124 (11% of reviewed papers).

125

126 According to the first methodological approach the geometry is directly defined based on
127 medical imaging through a segmentation and reconstruction process. Early approaches to
128 the FE modelling of the foot utilised X-ray images [12–15] but almost all reviewed studies
129 published after the year 2000 were based either on Magnetic Resonance Imaging (MRI), or
130 Computer Tomography (CT) images (S1 table). Sixty four percent (64%) of these studies

131 presented detailed 3D models of the entire foot [3,12–69] while 10% used detailed 3D
132 models focused on specific parts of the foot [4,5,70–77]. Fourteen percent (14%) of
133 reviewed studies developed 2D models of a cross-section of the foot based on a single
134 CT/MRI image [2,6,10,78–88]. Finally only one study (1% of reviewed papers) presented a
135 2D model of a cross-section of the foot (frontal cross- section of the heel) reconstructed
136 using ultrasound [89].

137

138 On the contrary idealised models of the foot entailed a simplified representation of
139 geometry either assuming some type of symmetry or by simulating the tissues of the foot
140 using basic geometrical shapes such as spheres, cylinders, etc. Eleven percent (11%) of the
141 reviewed studies followed this approach [7,90–99] out of which only one study presented a
142 3D model [98].

143

144 3.1.1. Design of 3D realistic models of the entire foot

145 Geometry reconstruction:

146 Realistic models of the entire foot are usually reconstructed either from CT, which is more
147 suited for imaging bones, or MRI which is more suited for soft tissues. CT and MRI were also
148 combined in three studies to produce a more detailed reconstruction of both bone and soft
149 tissues [30,51,69].

150

151 In the cases of CT and MRI, geometry reconstruction involves the segmentation of different
152 tissues (e.g. bone, ligaments etc.) in a series/stack of images that corresponds to different
153 sections/ slices of the foot. In most cases this process was performed manually or through
154 semi-automated procedures and the use of specialised software (e.g. Mimics, ScanIP etc.).

155 Based on that, it is clear that the reconstruction of the 3D geometry of the foot can be a
156 very labour intensive task. In order to address this problem Camacho et al. [100] presented
157 an automated method for the 3D reconstruction of the geometry of the bones of the foot
158 from CT images. An automatic outlining tool was used to establish the border of each bone
159 and this process was repeated for each slice containing the particular bone. The whole
160 process was repeated for each bone using the talus as reference to determine their relative
161 positions. The applicability of this method was demonstrated for a cadaveric foot and non-
162 weight bearing conditions. Finally it should be noted that in their paper Camacho et al. [100]
163 did not present information about the accuracy of their method.

164
165 A different solution to the same problem (i.e. the labour intensive nature of medical image
166 analysis) was presented by Lochner et al. [24]. The authors of this study developed a generic
167 anatomical foot model which was then modified to produce subject specific models. Skin
168 surface geometry of the subject's foot was scanned and anatomical landmarks were
169 identified and matched to those of the generic model reducing significantly the time needed
170 to generate a patient specific model of the physiologic foot [24]. The applicability of this
171 method was demonstrated using non-weight bearing imaging data from three subjects but
172 similar to Camacho et al. [100], its accuracy was again not validated. Another limitation of
173 this technique in the presented form is that it cannot be applied for "non-physiologic" feet
174 (e.g. feet with a deformity such as hallux valgus etc.). Despite their limitations the
175 aforementioned methods [24,100] highlight the need for automated algorithms to reduce
176 the amount of work needed for geometry reconstruction.

177

178 Besides the challenges related to the post processing of imaging data, the use of medical
179 imaging itself can also impose serious limitations to the applicability of such methods in the
180 clinical setting. More specifically one should also consider that both MRI and CT scanning
181 are lengthy and expensive processes. In the UK, the cost of performing an MRI or CT scan
182 can exceed £200 [101]. The costs normally relate to the scanning duration and the type of
183 scanner. Whilst in many cases patients would be offered MRI or CT scans as part of their
184 standard treatment plan, given the cost associated with these procedures it seems
185 unrealistic to request them for the sole purpose of FE modelling.

186

187 One of the main determinants in terms of the duration of the scanning process, is the
188 distance between imaged slices for the same total imaged area. Even though a variation of
189 different imaging protocols were used in the reviewed papers, in all cases, the foot was
190 imaged in the frontal plane and the distance between successive images/slices was less than
191 2 mm. Based on relevant experience within our team [102] such scanning process would
192 take around 30 min to be completed. Finally, in terms of CT, one should also consider the
193 risks associated with ionising radiation. .

194

195 Besides CT and MRI, X-ray imaging has also been used in a small number of studies
196 [14,15,103,104]. Although X-ray imaging has some advantages over CT/ MRI in terms of cost
197 and availability its use has been significantly limited mainly due to its significantly lower
198 accuracy. X-ray imaging generates projected images of all tissues in its field of view which
199 can make distinguishing different anatomical structures extremely difficult. As a result the
200 geometry of 3D models produced using X-rays had to be significantly simplified,
201 compromising their ability to produce reliable and clinically relevant results.

202

203 Simulation of foot function:

204 One of the main challenges for the FE modelling of the foot is the simulation of the function
205 of the foot's numerous joints. In order to address this challenge some authors bridged
206 bones at the joints using a relatively soft material [3,31] enabling some relative movement
207 between bones while others assumed contact between the opposite surfaces of the joints
208 [30,105]. The use of contact elements could enable a more realistic simulation of joint
209 function but at the same time it also significantly increases the computational cost and the
210 complexity of the analysis.

211

212 In any case, different levels of complexity in the simulation of joint function were needed for
213 studies with different objectives. The most elaborate and labour intensive approach for the
214 simulation of joints was presented by Isvilanonda et al. [30]. The authors of this study
215 combined CT with MRI images to get a more accurate reconstruction of both bone, which is
216 more clearly seen in CT, and cartilage, which is more clearly seen in MRI. The joint interface
217 conditions were simulated as contact with friction between deformable bodies (i.e.
218 cartilage). This approach was deemed necessary because the joint function was considered
219 to be very important for the purpose of this particular study, namely for the assessment of
220 joint angle correction that can be achieved by different surgical techniques in the case of
221 clawed hallux [30].

222

223 In total contrast to the aforementioned study Dai et al. [26] presented a 3D model of the
224 foot where most bones were fused. The skeleton was encapsulated inside a bulk soft tissue
225 which represented the outer morphology of the foot in detail. In order to recreate the

226 overall bending stiffness of the foot, partition layers were cut at the major joints of the foot
227 and linked with a material that simulated cartilage. In this case the aim of the FE
228 investigation was to assess the effect of wearing socks on plantar soft tissue loading (i.e.
229 plantar pressure and shear stress). For this purpose, the authors considered the overall
230 bending stiffness of the foot to be more important than the function of separate joints [26].

231

232 Meshing:

233 Unfortunately, only a few studies presented details about the type of elements and density
234 of mesh that was used. Based on the available information it appears that a 3D model of the
235 entire foot requires at least $\approx 36,000$ elements [59], while in some cases the total number of
236 elements can be as high as 400,000 [55]. Based on these figures and considering the non-
237 linear nature of most analyses (i.e. simulation of materials exhibiting non-linear mechanical
238 behaviour, contact etc.) it becomes evident that one of the main disadvantages of
239 geometrically detailed models is their high computational cost. Despite a clear trend for
240 increasing available computational power the use of computationally "expensive" models
241 would require specialised powerful computer units which would increase processing costs
242 and lead to an increased time lag between testing and getting the results.

243

244

245 3.1.2. Design of anatomically focused 3D models:

246 Geometry reconstruction:

247 In general, the focus of these analyses was on the plantar soft tissues of the forefoot
248 [4,73,76] or rear foot [5,70–72,74,75,77]. These models were again reconstructed from MRI
249 or CT images while the specific region that was modelled, was dictated by the aim of the

250 study. Scanning a smaller area of the foot might reduce the duration of the scanning
251 sequence but overall it is not expected to significantly reduce its cost.

252

253 Simulation of foot function:

254 Including only a part of foot anatomy into the model significantly limits the scenarios that
255 can be simulated. Based on that, it is no surprise that all studies included in this category
256 had objectives that enabled them to limit the analysis to very specific loading scenarios. For
257 example: Budhabhatti et al. [4] aimed to comparatively assess the efficiency of different
258 therapeutic interventions for plantar pressure reduction under the first ray of forefoot
259 during “push off to toe off phase” [4]. An interesting method for the calculation of the initial
260 configuration of the model was also presented here. More specifically, the authors of this
261 study calculated the initial angle of the 1st metatarsophalangeal Joint using an optimisation
262 process to minimise the difference between in vivo measured and numerically calculated
263 plantar pressure [4]. Similarly Fontanela et al. [75] designed a 3D model of the heel to
264 simulate heel strike for barefoot and shod conditions and to analyse the interaction
265 between the heel pad and different combinations of footwear materials.

266

267 Meshing:

268 In terms of meshing, only a handful of studies mentioned the number and type of element
269 that were used. More specifically Budhabhatti et al. [4] performed a mesh convergence
270 analysis and concluded that more than 10,000 8-node hexahedral elements were needed to
271 minimise the effect of mesh density on the calculated peak plantar pressures for push off.
272 On the other hand, Chokhandre et al. [72] used 30,576 hexahedral elements for their heel
273 model while Fontanella et al. [5] used 400,000. Based on these it appears that focusing on

274 specific areas of the foot doesn't necessarily lead to substantial reductions in the total
275 number of elements. However, limiting the simulation to specific regions of interest can
276 indeed reduce the overall computational cost of the analysis. For example focusing on the
277 heel eliminates the need for simulating joint function which, as mentioned earlier, can be
278 very computationally demanding.

279

280 3.1.3. Design of 3D idealised models:

281 To the knowledge of the authors of this review, the design and use of a geometrically
282 idealised 3D model of the foot has so far been presented only in one study by Spirka et al.
283 [98]. The aim of this study was to investigate the effect of different footwear designs on
284 plantar pressure reduction.

285

286 Geometry reconstruction:

287 Spirka et al [98] developed a 3D model of the metatarsal head area of the foot using a
288 combination of rigid spheres and cylinders to simulate the geometry of the metatarsal
289 bones. The dimensions and relative position of these shapes was measured from CT images.
290 More specifically, the radii of the spheres and lengths of the cylinders were equal to the
291 maximum measured widths of the metatarsal heads and the overall length of the metatarsal
292 bones respectively. The rigid bone models were linked with tension only springs simulating
293 ligaments [98]. The properties of the ligaments were assigned based on literature [40] and
294 their location based on anatomy software (Primal Pictures 3D Anatomy Software). The
295 model of the skeletal structure was embedded into a block of compliant material simulating
296 the plantar soft tissue. Although in this case the model was manually designed, the
297 presented methodology appears to have the potential to become automated.

298

299 Simulation of foot function:

300 The loading conditions of the metatarsal head area were simulated by directly loading each
301 metatarsal head sphere [98]. The amount of the imposed force on each sphere was first
302 estimated from plantar pressure measurements and then modified manually to minimise
303 the difference between the numerical and in vivo peak pressure under each metatarsal
304 head. Despite the simplified geometry and function of the foot model a comparison
305 between numerical simulation and in vivo measurements revealed a good agreement in
306 terms of pressure distribution. Even though this doesn't reduce the value of detailed
307 models, it highlights the importance of implementing simplifications that minimises the
308 labour intensity and computational cost of the model with minimum effect on the reliability
309 of results.

310

311 At this point it needs to be highlighted that the effect on reliability needs to be assessed in
312 the context of each specific application. For example, the modelling approach by Spirka et
313 al. [98] presented here appears to be accurate enough for applications where estimations of
314 plantar pressure are needed (e.g. informing the design of footwear interventions etc.).
315 However this approach [98] is unlikely to be accurate enough for applications focused on
316 internal tissue stresses.

317

318

319 Meshing:

320 Simplifications in terms of foot geometry and function can significantly reduce the amount
321 of work that is needed for the design and meshing of the model. Despite the fact that the

322 total number of elements used is not mentioned, it is easy to assume that significantly less
323 FEs are needed compared to a detailed 3D model of the same region therefore the
324 computational cost significantly decreases.

325

326

327 3.1.4. Design of 2D models:

328 Geometry reconstruction:

329 The studies included in this category focused on specific cross-sections of the foot and
330 reconstructed the geometry of the tissues of the foot based on a single 2D image. In order
331 to achieve that the authors of these studies assumed either plain strain [2,10,80,85] or plain
332 strain/ stress with thickness elasticity [6,89] or axisymmetry [7,96,97,99].

333

334 Yarnitzky et al. [93] aimed to develop a simulation technique for the patient specific
335 modelling of the heel pad and the real time calculation of its internal stresses and strains. To
336 achieve this they designed a 2D FE model of the heel based on simple measurements (i.e.
337 heel pad thickness, calcaneus curvature) on a sagittal X-ray of the foot. The 2D model of the
338 heel pad was then combined with a 2D analytical model of the entire foot for the calculation
339 of patient specific loading and the estimation of internal stresses. The accuracy of this
340 technique was assessed using a synthetic foot model comprising rigid plastic skeleton
341 embedded into silicon cast of the foot. These tests involved direct loading of the ankle joint
342 and the measurement of internal stresses of the silicon heel pad for different levels of
343 compression. According to the results presented by Yarnitzky et al. [93], the difference
344 between the measured internal stresses and the numerically estimated ones ranged
345 between 6.3% and 17%.

346

347 Whilst not all studies provided information about the source of the 2D image used to
348 reconstruct the geometry of the foot, it appears that most of them used images from MRI
349 [10,81] or CT [2] scans. Other than MRI and CT ultrasound imaging was also used in one
350 study [89]. More specifically, a frontal ultrasound image of the heel (B-mode imaging using a
351 linear array probe) at the area of the apex of the calcaneus was used to design a 2D model
352 (plane stress with thickness) of the heel comprising a rigid calcaneus and a deformable heel
353 pad. The geometry of the calcaneus and the thickness of the heel pad were reconstructed
354 using the ultrasound image. The thickness of the simulated slice was set equal to the
355 thickness of the ultrasound probe [89]. In contrast to CT and MRI, ultrasound is relatively
356 easy to use, safe (both for the patient and the operator) and its cost is low. On the other
357 hand ultrasound imaging offers relatively limited field of view with lower accuracy
358 compared to MRI or CT and the quality of the images can be strongly affected by scanning
359 technique. Another limitation of ultrasound is that it cannot penetrate bony structures and,
360 therefore, can image only their outer surfaces which makes it better suited for the study of
361 soft tissues (e.g. muscles, ligaments, tendons etc.). Besides its limitations ultrasound
362 imaging is a very good candidate for applications that are focused on soft tissues that are
363 close to skin such as the plantar soft tissues.

364

365

366 Simulation of foot function:

367 2D modelling imposes significant limitations to the load scenarios that can be simulated
368 because no out-of-plane forces or displacements can be imposed. Moreover, the joints (if
369 simulated) have to be simplified having only one rotational degree of freedom around an

370 axis which is always perpendicular to the simulation plane. A method to reduce the effect of
371 these limitations is to focus on specific areas/section of the foot and specific loading
372 conditions for which out-of-plane loading and movement is minimal. For example, Erdemir
373 et al. [6] used a 2D model of a slice of the metatarsal head area with the simulation plane
374 aligned with the axis of the metatarsal bone. This model was used to simulate a specific gait
375 event approximating the time of the second peak in vertical ground reaction force. For this
376 instance of gait it can be assumed that there are no off-plane forces, translations or
377 rotations.

378

379 Computational cost:

380 As one would expect the computational cost of 2D models of the foot is considerably lower
381 compared to 3D models. An extreme example for the low computational cost of 2D models
382 is the heel pad model of Yarnitzky et al. [93] where only 150 nodes were used.

383

384

385 3.2. Assignment of material properties

386 In the case of bones, cartilage, ligaments and tendons material properties were exclusively
387 assigned based on literature. On the contrary, the material properties of the soft tissues of
388 the sole of the foot (i.e. fat pad, skin etc.) were assigned using a combination of different
389 techniques including methods based on in vivo measurement for the calculation of subject
390 specific mechanical properties. The specific constitutive models used to simulate the
391 mechanical behaviour of the tissues of the foot and the methods for calculating and
392 assigning their material properties and mechanical coefficients are presented below.

393

394 The first thing that becomes clear from these analyses is the very wide range of values of
395 material properties/ coefficients that has been used to simulate the same tissue. Erdemir et
396 al. [7] investigated the effect of using non subject specific mechanical properties of plantar
397 soft tissue on peak plantar pressure and found that using material properties that are
398 averaged for a specific population may change peak plantar pressure by up to 7% compared
399 to using a subject specific mechanical properties. These results clearly highlight the effect of
400 the chosen materials properties on the obtained numerical results and the importance of
401 using patient specific ones when possible.

402

403

404 3.2.1 Material models

405 Bone and cartilage:

406 Bone tissue was modelled in almost all studies either as rigid or a homogenous linearly
407 elastic material with Young's modulus ranging from 7,000 MPa to 15,000 MPa. On the other
408 hand cartilage was only modelled in 55% of the reviewed studies and in almost all of them it
409 was simulated as linearly elastic with Young's modulus ranging from 1 MPa to 12MPa.
410 Cartilage was simulated as hyperelastic material only in 4% of studies [38,51,69,76] and as a
411 viscoelastic material only in one study (1% of reviewed papers) [62].

412

413 Whilst these studies covered a wide range of applications, it becomes clear that in
414 applications where bone and cartilage deformations are minimal (e.g. due to low magnitude
415 of loading) or irrelevant (e.g. studies focused on internal soft tissue stresses/ strains) the
416 shape of skeletal structures is far more important than the realistic simulation of their

417 mechanical behaviour. In contrast to the applications outlined above, one study aiming to
418 investigate the effect of impact loading on leg injury modelled both bone and cartilage as
419 viscoelastic materials [62]. Simulating the time-dependent aspects of the mechanical
420 behaviour of tissues can significantly increase the computational cost of the analysis.
421 Considering the aim of the aforementioned study and the highly dynamic nature of
422 simulated loads [62] it becomes clear that in this case the added computational cost is
423 necessary in order to achieve satisfactory accuracy.

424

425 Ligaments and tendons:

426 Ligaments were modelled in 62% of the reviewed studies. In the majority of these studies,
427 ligaments were assumed to be linearly elastic with Young's modulus ranging from 11.5 MPa
428 to 1,500 MPa. The non-linear mechanical behaviour of ligaments was taken into account
429 only in 6% of studies using a 5th order polynomial model [54,84,87,88] or as a viscoelastic
430 model [58,62] or fibre-reinforced viscohyperelastic model [51,69,76]. Most studies that
431 modelled ligaments paid special attention to the simulation of plantar fascia by using
432 different properties relative to the rest of the ligaments. Tendons were modelled only in
433 15% of studies and in all of these cases they were simulated as linearly elastic with Young's
434 modulus ranging from 15 MPa to 1,200 MPa.

435

436 Realistic simulation of the mechanical behaviour of ligaments and tendons is of paramount
437 importance in studies which focuses on (1) ligament or tendon biomechanics [51,106], (2)
438 the effect of pathological conditions [88] or (3) the efficiency of relevant treatments
439 [30,58]. Typical example of a FE analysis where the accurate simulation of ligament/ tendon

440 mechanical behaviour is very important is the study by Isvilanonda et al. [30] where two
441 different surgical techniques for the treatment of clawed hallux deformity were compared.
442 In this case, the ligaments and tendons were simulated as hyperelastic materials. However,
443 no clear evidence could be found which could indicate the best material model for each
444 specific application and there are cases where different material models have been used to
445 simulate similar scenarios. Considering the added computational cost and complexity that
446 results from the use of more elaborate material models it needs to be highlighted that in
447 every case the decision should be made through rigorous validation, based on the specific
448 aims of the study and the level of accuracy that is needed in order to achieve such aims.

449

450 Soft tissues:

451 Seventy seven percent (77%) of studies in total considered some type of bulk soft tissue to
452 simulate the combined mechanical behaviour of skin, fat and muscle. More specifically, 65%
453 modelled all three soft tissues together while 8% merged skin and fat in a single bulk tissue
454 and simulated muscle separately. On the contrary 4% of studies merged fatty layer and
455 muscle into a bulk tissue and simulated skin separately.

456

457 Even though some studies considered this bulk tissue to be linearly elastic ($E=0.15\text{MPa} -$
458 1.15MPa) [3,12–15,17,18,21–23,26–30,37,42,43,45,46,64–66,93,106–109] in most cases the
459 mechanical behaviour of the combined muscle and fatty layer was simulated as hyperplastic
460 using the Ogden material models. In all these cases bulk soft tissue was assumed to be
461 incompressible or nearly incompressible (Poisson's ratios of 0.45-0.49). The use of these
462 models required assigning values to a minimum number of two material coefficients in the

463 case of incompressible 1st order Ogden material [7,72] to a maximum number of six in the
464 case of 5th order polynomial material model [84,87].The viscous nature of the soft tissues of
465 the sole of the foot was also simulated using a visco-elastic [58,95] or a visco-hyperelastic
466 [70] constitutive model. In the aforementioned cases of visco-elastic and visco-hyperelastic
467 models a minimum number of two [95] to a maximum of five [70] coefficients had to be
468 defined.

469

470

471 Skin was simulated as a separate tissue in 20% of reviewed studies [2,5,31,36,51,56,59–
472 61,69,71,73–77,83,85,94] . In these studies skin was mainly simulated as isotropic
473 hyperplastic using the Ogden [71,73,77,83], Neo-Hookean [60,61] Jamus-Green-Simpson
474 [94] or 2nd order polynomial [2,56] material models. A more elaborate model was used by
475 Fontanella et al. and also Forestiero et al. who simulated skin as fibre-reinforced anisotropic
476 hyperelastic material [5,69,75,76]. On the contrary a more simplified approach was followed
477 by Shin et al. and Luboz et al. who simulated skin as having a linearly elastic mechanical
478 behaviour [31,59]. The number of material coefficients that the authors had to define for
479 the aforementioned models was one for incompressible Neo-Hookean, two for
480 incompressible Ogden hyperelastic [71,73,77], five coefficients for the Jamus-Green-
481 Simpson and six coefficients for the 2nd order polynomial [2] and the fibre reinforced
482 hyperelastic material models [5,75,76].

483

484 Fat pad was simulated as a separate tissue in 19% of reviewed studies [2,5,31,36,51,59–
485 61,69,71,73–77,83,85,94]. In most of these studies fat tissue was simulated using the Ogden
486 hyperplastic model while its visco-hyperelastic nature was only simulated in 5% of studies

487 [5,51,69,75,76]. The visco-hyperelastic model that was used in these cases required
488 assigning values to twelve material coefficients in total [5,51,69,75,76].

489

490 Muscle was simulated as a separate tissue only in 9% of studies [19,38,59–62,73,86] using
491 either the Ogden [73] or the Mooney Rivlin [19,38] or neo-Hookean [60,61] models. In a
492 more simple approach Luboz et al. [59] simulated muscle as linearly elastic.

493

494 A critical analysis indicates that studies focused on bone fracture, fixation and healing
495 [19,27,86] or the biomechanics of ligaments and tendons [21,22,30,37,38,45,65,109] are
496 unlikely to need nonlinear material models for the simulation of plantar soft tissue
497 mechanical behaviour. In these cases the assumption of linear elasticity appears to offer
498 satisfactory accuracy for the intended use of the models. In other cases and especially
499 where the focus is on internal plantar soft tissue stresses/ strains the use of more elaborate
500 material models appears to be very significant.

501

502 In the case where a more accurate simulation of plantar soft tissue biomechanics is needed,
503 the most commonly used material model is the 1st order Ogden hyperelastic model. This
504 model appears to enable accurate simulation of the nonlinear nature of the mechanical
505 behaviour of plantar soft tissue and reliable estimation of plantar pressure with the
506 minimum number of material coefficients [7,72,89,110,111]

507

508 3.2.2 Subject specific material properties

509 Despite the fact that for most tissues (e.g. ligaments, tendons, cartilage etc.) the calculation
510 of subject specific mechanical properties is extremely difficult, the reviewed studies include

511 in vivo measurement based methods that enable the calculation of subject specific
512 properties for the soft tissues of the sole of the foot. These methods are implemented in
513 two steps namely: in vivo testing and coefficients calculation.

514

515 In vivo testing:

516 The two most commonly used in vivo tests for the material characterisation of plantar soft
517 tissue is indentation [7,68,77,82,89,94] and compression [5,73]. In the case of indentation,
518 a rigid indenter with dimensions that are significantly smaller than the tested area is pressed
519 against the plantar aspect of the foot. The applied force is measured using a load sensor
520 which is in series with the indenter while tissue deformation is assessed either based on
521 indenter displacement [12,77] or the real-time measurement of indenter-to-bone distance
522 [7,68,82,89]. In the latter case the plantar soft tissue is loaded using an ultrasound probe
523 which plays the role of the indenter (i.e. ultrasound indentation).

524

525 In the case of compression, the rigid surface that is used to load the foot has similar or
526 larger area than the loaded area of the foot. Similar to indentation, in this case tissue
527 deformation is either calculated based on the displacement of the compression plate [5] or
528 directly measured using medical imaging [73]. The effect of the size of indenter on the
529 reliability of indentation results was numerically investigated by Spears et al. [112] who
530 concluded that indenters with bigger footprints can produce more reliable and robust
531 measurements of the stiffness of the heel-pad.

532

533

534 Coefficients' calculation:

535 The most common technique for the calculation of the nonlinear material coefficients of
536 plantar soft tissue is inverse FE analysis [7,20,73,89,94,99]. According to this method a FE
537 model of the in vivo test is used to calculate the values of the tissues' material coefficients
538 that minimise the difference between in vivo and numerical results. To this end, Erdemir et
539 al. [7] performed ultrasound indentation tests at the heel using a cylindrical indenter. These
540 tests were then simulated using axisymmetric FE models comprising a bulk soft tissue with
541 subject specific thickness. An optimisation algorithm was utilised to find the values of two
542 nonlinear material coefficients (Ogden 1st order) that minimise the difference between the
543 numerical and in vivo force/deformation curves of the indentation test [7]. In order to
544 improve the subject specificity of the inverse engineering process Chatzistergos et al. [89]
545 loaded the foot using a linear array ultrasound probe and reconstructed the geometry of the
546 calcaneus in the field of view from B-mode images. In this case the indentation test was
547 simulated using a plane stress with thickness model comprising a bulk soft tissue with
548 subject specific thickness and geometry [89]. An optimisation algorithm was used to inverse
549 engineer the material coefficients of heel-pad.

550

551 A more elaborate approach was followed by Petre et al. [73] who used a custom made
552 device to compress the forefoot inside an MRI scanner. The compression test was then
553 simulated using subject specific 3D FE models of the forefoot comprising rigid bones and
554 layers of different soft tissues (i.e. skin, fat and muscle). The geometry of these models was
555 reconstructed from the MRI images of the unloaded foot while the MRI images of the
556 loaded foot were used to assess internal deformations of different layers of soft tissues. At
557 the end, an optimisation algorithm was used to minimise the difference between the
558 numerically calculated and the in vivo measured internal deformations. This approach

559 enabled the calculation of six material coefficients in total (i.e. two coefficients per tissue
560 layer) [73]. The results of this study also indicated that realistic representation of the
561 internal structure of plantar soft tissues is needed in order to achieve a more accurate
562 estimation of internal tissue stresses/ strains [73]. This finding highlights the importance of
563 simulating the inhomogeneity of plantar soft tissue in order to achieve satisfactory accuracy
564 in applications that are focused on the accurate estimation of internal plantar soft tissue
565 stresses/ strains.

566

567 It is clear from the aforementioned studies that there is a limit to the number of coefficients
568 that can be inverse engineered from indentation or compression tests. Moreover, increasing
569 the material coefficients that need to be calculated can also significantly increase the overall
570 analysis time of the inverse engineering process [111] by increasing the number of iterations
571 that are needed to reach final solution. To overcome these problems some authors
572 combined in vivo testing with the use of in vitro data from literature [5,77]. For example,
573 Fontanella et al. [5,113] used data from in vitro tests to get a first estimation of the twelve
574 coefficients for their visco-hyper-elastic model of the heel pad and then used in vivo
575 compression tests performed at different loading rates to adapt the values of six of these
576 coefficients.

577

578 A significantly more simple approach was followed by Thomas et al. [12] in a study aiming to
579 assess the effect of stiffening of plantar soft tissue on its internal stresses in people with
580 diabetes. For this purpose a standardised durometer was used to measure Shore hardness
581 at the heel. The elasticity modulus of heel pad was directly estimated from Shore hardness
582 using a previously published relationship that links the shore hardness of cartilage to its

583 modulus of elasticity [114]. Even though this technique is by far the most easy to use, it is
584 non-invasive and computationally efficient it is highly unlikely that it can achieve the desired
585 levels of accuracy especially in terms of estimation of internal tissue stresses/ strains.

586

587 Considering the challenges around the calculation of subject specific material properties, it
588 is clear that the potential for clinically applicable modelling is significantly enhanced in
589 applications where the required accuracy can be achieved with the use of generic or
590 population specific properties instead of subject specific ones [115]. An application of FE
591 modelling that appears to fulfil this criterion is the optimisation of the cushioning properties
592 of bespoke insoles [89]. In this context, a numerical study performed by Chatzistergos et al.
593 [89] indicated that the stiffness of an insole that minimises plantar pressure is not affected
594 by the stiffness of plantar soft tissue. In contrast to patient specific tissue mechanical
595 properties patient specific loading was found to have a very strong effect on the optimal
596 cushioning properties of insoles [89].

597

598 3.3 Loading:

599 Loading within the reviewed studies, in the main, was applied in the form of external (i.e.
600 ground reaction force) or internal forces (i.e. muscle forces) or a combination of both (S1
601 table). The values of these forces were calculated either based on body mass, or in vivo
602 measurements or using musculoskeletal modelling.

603

604

605

606

607 3.3.1 loading scaled based on body mass

608 Forty three percent (43%) of the reviewed studies calculated the forces that are imposed on
609 the foot model as a percentage of body weight (BW) based on literature. Most of the
610 studies simulated balanced standing by applying 50% of BW on the centre of pressure or the
611 ankle joint. Studies that considered muscle forces applied 25% BW to the Achilles tendon
612 [16,17,21,27,28,32,34,44–46]. The reported in literature percent of BW that is applied to the
613 Achilles tendon was increased to 37.5% BW in two studies to improve agreement with in
614 vivo measurements in terms of plantar pressure [23,65].

615

616 Another technique for the simulation of balanced standing is to separately calculate the
617 loading that is imposed to different parts of the foot. This technique was used in the case of
618 2D models simulating different rays of the foot [2,84,87,88] but also in the case of 3D
619 models [19,38] aiming at a more realistic distribution of foot internal loading. In these cases
620 the calculation of individual loading for each foot array was based on data from Simkin [116]
621 according to which the total load carried by the foot can be distributed as 25%, 19%, 19%,
622 19%, 18% from first to fifth ray respectively [116].

623

624 3.3.2 Loading based on in vivo measurements:

625 Twenty six percent (26%) of the reviewed studies directly measured ground reaction forces
626 using force plates, pressure mats or in-shoe pressure sensors to define the magnitude of the
627 imposed loading. Assigning loading directly from measured ground reaction forces appears
628 to be very relevant for studies focusing on specific regions of the foot and specific phases of
629 gait offering reliable estimations of plantar pressure. A typical example for this approach is

630 the study by Budhabhatti et al. [4] where subject specific toe off ground reaction forces
631 were measured using a force plate and then were applied to a subject specific 3D model [4].

632

633 Moreover, the use of accurate measurements of subject specific loading seems to be very
634 relevant for studies focused on foot/ footwear interactions and plantar pressure reduction.

635 As mentioned earlier this was highlighted in a numerical study by Chatzistergos et al. [89]
636 where loading magnitude was found to be the most important factor for the optimisation of
637 the cushioning properties of insole materials.

638

639 In order to calculate subject specific internal forces (i.e. ankle joint forces and the plantar
640 fascia tension) Yarnitzky et al. [93] combined in-shoe measurements with an analytical
641 model of the foot. The authors aimed to develop a simulation technique for the patient
642 specific modelling of the heel pad and the real time calculation of its internal stresses and
643 strains. For this purpose they designed a 2D FE model of the heel based on simple
644 measurements on a sagittal X-ray of the foot (i.e. heel pad thickness, calcaneus curvature).
645 The 2D model of the heel pad was then combined with a 2D analytical model of the entire
646 foot which was used to estimate the force vectors in the Achilles tendon, plantar fascia,
647 plantar ligament and tibio-talus joint [93].

648

649 All FE analyses are based on either assumed or measured loads to calculate internal tissue
650 stresses and strains. This fundamental characteristic of FE analysis means that FE models
651 cannot directly predict adaptations in gait and therefore in tissue loading as a result of
652 altered internal tissue properties or stresses/strains. In order to overcome this limitation,
653 Hollaran et al. [78,80] combined musculoskeletal modelling with optimal control and FE

654 modelling. More specifically the authors of these studies used a 2D musculoskeletal model
655 of trunk and lower limbs comprising seven rigid segments, eight muscle groups which were
656 coupled with a 2D (plain strain) model of the 2nd ray of the foot. The two models were
657 coupled at the ankle joint with the musculoskeletal model passing to the FE model the
658 vertical position and orientation of the ankle joint and the FE analysis calculating and
659 returning to the musculoskeletal model the ankle joint reaction forces. The prediction of
660 changes in gait was performed using an optimal control algorithm which searched for gait
661 patterns that satisfy the conditions of the problem (e.g. periodicity, constant walking speed
662 etc.) and at the same time minimised a cost function. This cost function was defined in a
663 way that enabled among others the minimisation of muscle “fatigue” and the minimisation
664 of the intensity of plantar soft tissue loading. Despite limitations such as high
665 computational cost (i.e. reported computation time of 10-14 days) this novel approach
666 highlights the potential of combining different modelling regimes (i.e. musculoskeletal
667 modelling with optimal control and FE modelling) to predict adaptations in gait due to
668 mechanical changes in tissues, or to indicate how gait could be altered to change the way
669 tissues are loaded to prevent injuries or promote rehabilitation. Despite this there is no
670 information provided on the in vivo validation of this method.

671

672

673 3.4 FE model validation:

674 Validation is of paramount importance for any clinically relevant application of FE modelling
675 but at the same time it remains one of the most challenging aspects of computational
676 biomechanics. Indicative of this is the fact that 44% of the reviewed studies did not present
677 any kind of validation (S1 table). The studies that did include validation (56%) compared

678 numerical results against in vivo or in-vitro experimental data (i.e. direct validation) or
679 against data from literature (i.e. indirect validation).

680

681 In the case of indirect validation (6% of the reviewed studies) the numerically estimated
682 plantar pressures [50] or stress/strain behaviour of specific tissues [2,31,35,93] was
683 compared to respective data from literature [2,31,35,38,50,93].

684

685 In the case of direct validation against in vivo data, the majority of studies used barefoot or
686 in-shoe plantar pressure distribution and/or peak plantar pressure. Besides that, one study
687 compared numerically calculated ground reaction forces against in vivo measured ones [88]
688 and one more study compared numerical and experimental displacements of specific bones
689 using direct motion capture and reflective markers [46].

690

691

692 4. Discussion

693 This review highlights that a number of fundamental challenges still exist and a considerable
694 progress is still required before patient specific FE analysis can become a clinical tool for the
695 management of diabetic foot or other foot pathologies. The key challenges in terms of
696 model design, material properties assignment and loading are described below and possible
697 available solutions are discussed. Considering the fact that achieving satisfactory levels of
698 accuracy is the ultimate deciding factor for the clinical applicability of any numerical
699 technique, methods for direct validation are discussed separately at the end of this section.

700

701

702 4.1 Model design

703 The first key challenge towards clinically applicable FE modelling is collecting reliable
704 information for geometry design/ reconstruction in a cost effective and non-invasive way.
705 Based on the reviewed studies, it is clear that the two most commonly used imaging
706 modalities for this purpose is CT and MRI. This is because CT and MRI offer superior image
707 quality enabling the accurate reconstruction of bone or soft tissue geometry respectively.
708 Based on that it is clear that in the case of applications and pathological conditions where CT
709 and/or MRI are already included into the patients' standard treatment their use to support
710 FE modelling would clearly be the best option.

711

712 Besides that, in cases where CT and/or MRI are not part of the standard treatment plan of
713 patients requesting them solely for modelling purposes seems impractical. In these cases
714 ultrasound imaging with its low cost, low risk for patients and high availability in clinics
715 appears to be the best alternative imaging modality to support FE modelling [89]. Considering
716 the limitations of ultrasound in terms of depth of field-of-view, contrast and bone imaging it
717 becomes clear that its use will have to be restricted to applications focusing on soft tissues
718 close to the surface of the foot, such as skin, fat pad etc. Moreover, concerns about user
719 dependency will also have to be addressed. The development of automated ultrasound
720 scanning systems for the foot can enhance reproducibility and minimise user dependency
721 phenomena.

722

723 X-ray and surface topography have also been used to reconstruct the geometry of the foot.
724 In the case of X-ray risks with regards to the use of ionising radiation and the difficulties in
725 distinguishing overlapping anatomical structures have significantly limited its usage. On the
726 other hand surface topography offers a relatively quick, cost effective and accurate
727 reconstruction of the 3D geometry of the external surfaces of the foot. However the fact
728 that it cannot offer any information on the internal structure of the tissues of the foot
729 makes its stand-alone use for the design of FE models of non-physiologic feet very
730 challenging.

731

732 The second key challenge is being able to accurately reconstruct tissue geometry in a non-
733 labour intensive way and without the need for specialist knowledge. Most of the reviewed
734 studies employed specialised software for the manual segmentation and 3D reconstruction
735 of tissue geometry. In contrast to this approach reliable automated techniques are required
736 to reconstruct tissue geometry with minimum user input. For this purpose two automated
737 techniques for the design of 3D models of the foot were identified. According to the first
738 one, an automatic outlining tool was used to segment bones in a series/stack of CT images
739 produce 3D objects by combining the bone outlines of successive slices [100]. The second
740 solution employed a generic model of the foot which was modified and adapted to match
741 the external geometry of the subject's foot [24]. Although these two studies highlight the
742 potential for automated geometry reconstruction techniques, to the knowledge of the
743 authors of this review, these methods have not been yet validated nor used in big cohort
744 studies indicating that substantial further development is needed.

745

746 The third key challenge related to model design is minimising the computational cost
747 associated with FE analyses to enable immediate feedback on results without the use of
748 specialised high performance computational units.

749

750 The computational cost of FE simulations increases with the size of the model and the
751 complexity of the analysis. In general, the size of a FE model corresponds to the total
752 number of equations that need to be solved in each step/ iteration (i.e. total number of
753 degrees of freedom), which in turn depends on the type and total number of elements in
754 the model. On the other hand complexity is linked to the number of steps/ iterations that
755 are needed to get the final results of the analysis (i.e. the number of times that the
756 aforementioned equations need to be solved). Starting from a simple linear analysis where
757 solution is achieved in one step/ iteration the simulation of any nonlinear or time
758 dependent phenomenon can significantly increase computational cost by significantly
759 increasing the number of solution steps/ iterations that are needed in order to reach the
760 final solution. Specifically in the case of the reviewed studies, the computational cost is
761 significantly increased by the use of materials with nonlinear and/or time dependent
762 mechanical behaviour (e.g. hyperelastic materials, viscoelastic etc.) and by the use of
763 contact elements.

764

765 Despite the fact that not all studies provided information about the computational cost of
766 their models it is clear that detailed 3D models of the entire foot will include a significant
767 number of degrees of freedom. This, combined with the non-linear nature of the analyses

768 and possible need for contact elements to simulate joint function will make performing the
769 analyses very challenging without using specialised high performance systems. Two generic
770 approaches were identified to reduce computational cost, namely the design of
771 anatomically focused models or the design of simplified/ idealised ones. The studies
772 following the first approach designed highly specialised models of parts of the foot (e.g.
773 heel) simulating very specific loading scenarios (e.g. heel strike). By significantly limiting the
774 range of scenarios that the model can simulate, the authors of these studies were able to
775 design anatomically detailed models of parts of the foot and reduce the models' degrees of
776 freedom [4,5,70–77] and in some cases eliminate the need for simulating joint function
777 [5,70–72,74,75,77]. Based on the published data it is clear that drastic reduction in
778 computational cost can only be achieved through radical simplifications in tissue geometry
779 and foot function [26,89,93,98].

780

781 At this point it needs to be re-iterated that accuracy is the ultimate deciding factor for
782 clinical applicability. Considering that accuracy and minimal computational costs are two
783 objectives that are usually mutually exclusive means that the actual target for future
784 developments in this field should be finding methods that can achieve satisfactory accuracy
785 with the minimum possible computational cost and not simply minimising computational
786 cost.

787

788

789

790 4.2 Assignment of material properties

791 All biological tissues exhibit complex non-linear and time depended mechanical behaviour
792 which makes their simulation inherently difficult. The majority of the reviewed studies
793 assigned material properties based on literature. Whilst identifying the right material model
794 and properties from the wide range of possible options in literature could be adequately
795 difficult the real challenge is being able to estimate material properties on a patient specific
796 basis. To achieve that, a combination of in vivo mechanical testing and advanced
797 computational and/ or mathematical analysis techniques is required. Moreover it is clear
798 that in order for these techniques to be applicable in the clinic, in vivo mechanical testing
799 will have to be non-invasive and easy to perform in a clinical setting and the techniques for
800 the calculation of material properties should be robust and fast.

801

802 In this context, the reviewed studies included methods that can only be used to calculate
803 patient specific material properties of plantar soft tissues. These methods were based on
804 two similar types of non-invasive mechanical tests, namely indentation and compression,
805 using custom made loading devices designed specifically for this purpose. The combined use
806 of these loading devices with MRI or ultrasound imaging, can significantly enhance the
807 reliability of the measurements by enabling the direct measurement of internal tissue
808 deformations [7,73,89]. Moreover the use of medical imaging opens the way for separate
809 material characterisation of different tissues, namely skin, fat etc. instead of the common
810 practice of characterising only a bulk plantar soft tissue [73]. To this end, the techniques like
811 ultrasound elastography may be used to differentiate between the different layers of soft
812 tissue in terms of the differences in density and deformability.

813

814 In addition, these studies highlight the potential for patient specific characterisation of
815 plantar soft tissue mechanical behaviour [7,73,89]. However the actual techniques used,
816 appear to be better suited for lab-based applications rather than for use in clinics. Building
817 on the existing techniques special attention needs to be paid to develop affordable in vivo
818 testing systems that are safe and easy to use in the clinic. Specialised devices that require
819 the patient to stand or rest their feet on a scanning surface to produce a map of the
820 mechanical properties of plantar soft tissues would have significantly higher chances of
821 being integrated into clinical practice compared to existing compression or indentation
822 devices. Considering recent advances in the fields of weight bearing foot scanners,
823 ultrasound imaging and elastography the development of such scanning device seems
824 feasible.

825

826 In terms of the computational aspects of tissue mechanical characterisation, the reviewed
827 studies highlighted the use of inverse engineering from in vivo testing mainly using
828 optimisation driven procedures. These iterative methods are associated with high
829 computational cost which can significantly limit their clinical applicability. A possible
830 solution to this problem is the use of surrogate models that can be trained to predict the
831 output of FE analyses thus considerably reducing the computational cost of the inverse
832 engineering process [117]. At this point, it needs to be stressed out that the reliability of
833 these surrogate models is still to be proven, especially in wide cohorts, therefore it is fair to
834 say that a considerable amount of work is still needed to ensure validity and accuracy before
835 deciding the applicability of such techniques in the clinic.

836 4.3 Loading

837 One of the main challenges in terms of defining boundary conditions and loading for the
838 models is being able to assign clinically relevant loading without the need for specialised
839 equipment and time-consuming measurements. According to literature, the simplest
840 methods to calculate loading appear to be a scaling based on literature or previous
841 normative measurements using the patient's body weight. However, it is clear that
842 calculating loading using this approach would limit the patient specificity of the analysis.

843

844 In cases where accurate measurements of truly patient specific loading are critical for the
845 reliability of the analysis, measurements of ground reaction forces using force plates,
846 pressure mats or in-shoe pressure sensors could be used to directly inform loading in the
847 form of externally applied forces [75] or a combination of external and internal forces [93].

848

849 4.4 Validation

850 The ultimate challenge for the implementation of any FE modelling system into clinical
851 practice is to ensure that it can produce reliable models for any person that belongs in the
852 population for which it was developed. This means that the accuracy of every part of the
853 modelling process as well as of the entire process as a whole will have to be assessed in
854 wide cohort studies to validate their accuracy for populations rather than just for
855 individuals. These validation tests will not have to be implemented in the clinic as part of
856 day-to-day practice which opens the way for more elaborate, thorough and at the same
857 time time-consuming and expensive approaches, such as the combined use of medical
858 imaging and custom loading devices to study internal tissue deformations [9,118].

859

860 Besides validating the ability of the entire process to generate reliable models for specific
861 populations, additional validation protocols for each individual patient will also be needed.

862 In this case simpler validation protocols will be needed that can be implemented in the clinic
863 without significantly increasing the time and cost of the whole process. For this purpose
864 more basic pressure based validation approaches could be used (see section 3.4).

865

866

867 5. Conclusion

868 The review clearly highlights the potential for the currently available models to be utilised in
869 a clinically applicable fashion. This is specifically the case where the FE models were used to
870 identify the mechanical properties of the plantar soft tissue for diagnostic purposes and in
871 identifying the effect of footwear on an individualised basis. This has been facilitated by the
872 practicality of using simplified geometry (that is not necessarily feasible in other areas of FE
873 application i.e. corrective bone surgeries) which can significantly reduce computational cost
874 as well as the amount of information that is needed for model design. Furthermore the
875 ability to quantify subject specific geometry and material properties through techniques
876 such as ultrasound elastography that can be easily implemented in a clinic promises new
877 possibilities in the area of diagnostics and prescription.

878

879 Finally, this review highlights the need for thorough and extensive validation of each
880 individual step of the modelling process as well as the validation of the final integrated
881 system. As indicated in this review, the ultimate challenge for the implementation of any

882 computational system into clinical practice will be to ensure its accuracy not just for a small
883 group of people but for the entire population for which it was developed.

884

885

886 **References:**

- 887 [1] Atlas E, Yizhar Z, Gefen A. The Diabetic Foot Load Monitor: A Portable Device for
888 Real-Time Subject-Specific Measurements of Deep Plantar Tissue Stresses During
889 Gait. *J Med Device* 2008;2:11005.
- 890 [2] Agić A, Nikolić V, Mijović B, Reischl U. Biomechanical model of the diabetic foot. *Coll*
891 *Antropol* 2008;32:881–6.
- 892 [3] Chen W-P, Ju C-W, Tang F-T. Effects of total contact insoles on the plantar stress
893 redistribution: a finite element analysis. *Clin Biomech* 2003;18:S17–24.
- 894 [4] Budhabhatti SP, Erdemir A, Petre M, Sferra J, Donley B, Cavanagh PR. Finite element
895 modeling of the first ray of the foot: a tool for the design of interventions. *J Biomech*
896 *Eng* 2007;129:750–6.
- 897 [5] Fontanella CGG, Matteoli S, Carniel EL, Wilhjelm JE, Virga a., Corvi a., et al.
898 Investigation on the load-displacement curves of a human healthy heel pad: In vivo
899 compression data compared to numerical results. *Med Eng Phys* 2012;34:1253–9.
- 900 [6] Erdemir A, Saucerman JJ, Lemmon D, Loppnow B, Turso B, Ulbrecht JS, et al. Local
901 plantar pressure relief in therapeutic footwear: design guidelines from finite element
902 models. *J Biomech* 2005;38:1798–806.
- 903 [7] Erdemir A, Viveiros ML, Ulbrecht JS, Cavanagh PR. An inverse finite-element model of
904 heel-pad indentation. *J Biomech* 2006;39:1279–86.
- 905 [8] Miller-Young JE, Duncan NA, Baroud G. Material properties of the human calcaneal
906 fat pad in compression: experiment and theory. *J Biomech* 2002;35:1523–31.
- 907 [9] Petre MT, Erdemir A, Cavanagh PR. An MRI-compatible foot-loading device for
908 assessment of internal tissue deformation. *J Biomech* 2008;41:470–4.
- 909 [10] Goske S, Erdemir A, Petre M, Budhabhatti S, Cavanagh PR. Reduction of plantar heel
910 pressures: Insole design using finite element analysis. *J Biomech* 2006;39:2363–70.
- 911 [11] Telfer S, Erdemir A, Woodburn J, Cavanagh PR. What Has Finite Element Analysis
912 Taught Us about Diabetic Foot Disease and Its Management? A Systematic Review.
913 *PLoS One* 2014;9:e109994.
- 914 [12] Thomas VJ, Patil KM, Radhakrishnan S. Three-dimensional stress analysis for the
915 mechanics of plantar ulcers in diabetic neuropathy. *Med Biol Eng Comput*
916 2004;42:230–5.
- 917 [13] Jacob S, Patil MKM. Three-dimensional Foot Modeling and Analysis of Stresses in
918 Normal and Early Stage Hansen ' s Disease with Muscle Paralysis. *J Rehabil Res Dev*

- 919 1999;36:252–63.
- 920 [14] Jacob S, Patil MK. Stress analysis in three-dimensional foot models of normal and
921 diabetic neuropathy. *Front Med Biol Eng* 1999;9:211–27.
- 922 [15] Patil KM, Jacob S. Mechanics of tarsal disintegration and plantar ulcers in leprosy by
923 stress analysis in three dimensional foot models. *Indian J Lepr* 2000;72:69–86.
- 924 [16] Cheung JTM, Zhang M. A 3-dimensional finite element model of the human foot and
925 ankle for insole design. *Arch Phys Med Rehabil* 2005;86:353–8.
- 926 [17] Sun P, Shih S, Chen Y, Hsu Y, Yang R, Chen C. Biomechanical analysis of foot with
927 different foot arch heights: a finite element analysis. *Comput Methods Biomech
928 Biomed Engin* 2012;15:563–9.
- 929 [18] Yu J, Cheung JT-M, Wong DW-C, Cong Y, Zhang M. Biomechanical simulation of high-
930 heeled shoe donning and walking. *J Biomech* 2013;46:2067–74.
- 931 [19] Wu L, Zhong S, Zheng R, Qu J, Ding Z, Tang M, et al. Clinical significance of
932 musculoskeletal finite element model of the second and the fifth foot ray with
933 metatarsal cavities and calcaneal sinus. *Surg Radiol Anat* 2007;29:561–7.
- 934 [20] Gu YD, Ren XJ, Li JS, Lake MJ, Zhang QY, Zeng YJ. Computer simulation of stress
935 distribution in the metatarsals at different inversion landing angles using the finite
936 element method. *Int Orthop* 2010;34:669–76.
- 937 [21] Cheung J, An K, Zhang M. Consequences of partial and total plantar fascia release: a
938 finite element study. *Foot Ankle Int* 2006;27:125–32.
- 939 [22] Liang J, Yang Y, Yu G, Niu W, Wang Y. Deformation and stress distribution of the
940 human foot after plantar ligaments release: a cadaveric study and finite element
941 analysis. *Sci China Life Sci* 2011;54:267–71.
- 942 [23] Yu J, Cheung JT-M, Fan Y, Zhang Y, Leung AK-L, Zhang M. Development of a finite
943 element model of female foot for high-heeled shoe design. *Clin Biomech (Bristol,
944 Avon)* 2008;23 Suppl 1:S31-8.
- 945 [24] Lochner SJ, Huissoon JP, Bedi SS. Development of a patient-specific anatomical foot
946 model from structured light scan data. *Comput Methods Biomech Biomed Engin*
947 2014;17:1198–205.
- 948 [25] Cheung JT-M, Zhang M, An K-N. Effect of Achilles tendon loading on plantar fascia
949 tension in the standing foot. *Clin Biomech (Bristol, Avon)* 2006;21:194–203.
- 950 [26] Dai X-Q, Li Y, Zhang M, Cheung JT-M. Effect of sock on biomechanical responses of
951 foot during walking. *Clin Biomech (Bristol, Avon)* 2006;21:314–21.
- 952 [27] Brilakis E, Kaselouris E, Xypnitos F, Provatidis CG, Efstathopoulos N. Effects of foot
953 posture on fifth metatarsal fracture healing: a finite element study. *J Foot Ankle Surg*
954 2012;51:720–8.
- 955 [28] Chen W-M, Lee T, Lee PV-S, Lee JW, Lee S-J. Effects of internal stress concentrations
956 in plantar soft-tissue--A preliminary three-dimensional finite element analysis. *Med
957 Eng Phys* 2010;32:324–31.
- 958 [29] Cheung JT-M, Zhang M, An K-NN, Tak-Man Cheung J, Zhang M, An K-NN. Effects of
959 plantar fascia stiffness on the biomechanical responses of the ankle-foot complex.

- 960 Clin Biomech (Bristol, Avon) 2004;19:839–46.
- 961 [30] Isvilanonda V, Dengler E, Iaquinto JM, Sangeorzan BJ, Ledoux WR. Finite element
962 analysis of the foot: model validation and comparison between two common
963 treatments of the clawed hallux deformity. Clin Biomech (Bristol, Avon) 2012;27:837–
964 44.
- 965 [31] Shin J, Yue N, Untaroiu CD. A finite element model of the foot and ankle for
966 automotive impact applications. Ann Biomed Eng 2012;40:2519–31.
- 967 [32] Qiu T-X, Teo E-C, Yan Y-B, Lei W. Finite element modeling of a 3D coupled foot-boot
968 model. Med Eng Phys 2011;33:1228–33.
- 969 [33] Gu YD, Li JS, Lake MJ, Zeng YJ, Ren XJ, Li ZY. Image-based midsole insert design and
970 the material effects on heel plantar pressure distribution during simulated walking
971 loads. Comput Methods Biomech Biomed Engin 2011;14:747–53.
- 972 [34] Bayod J, Becerro-de-Bengoa-Vallejo R, Losa-Iglesias ME, Doblaré M. Mechanical
973 stress redistribution in the calcaneus after autologous bone harvesting. J Biomech
974 2012;45:1219–26.
- 975 [35] Jamshidi N, Hanife H, Rostami M, Najarian S, Menhaj MB, Saadatinia M, et al.
976 Modelling the interaction of ankle-foot orthosis and foot by finite element methods
977 to design an optimized sole in steppage gait. J Med Eng Technol 2010;34:116–23.
- 978 [36] Agić A, Nikolić T, Mijović B. Multiscale phenomena related to diabetic foot. Coll
979 Antropol 2011;35:419–25.
- 980 [37] Spyrou L a, Aravas N. Muscle-driven finite element simulation of human foot
981 movements. Comput Methods Biomech Biomed Engin 2012;15:925–34.
- 982 [38] Wu L. Nonlinear finite element analysis for musculoskeletal biomechanics of medial
983 and lateral plantar longitudinal arch of Virtual Chinese Human after plantar
984 ligamentous structure failures. Clin Biomech (Bristol, Avon) 2007;22:221–9.
- 985 [39] Actis RL, Ventura LB, Smith KE, Commean PK, Lott DJ, Pilgram TK, et al. Numerical
986 simulation of the plantar pressure distribution in the diabetic foot during the push-off
987 stance. Med Biol Eng Comput 2006;44:653–63.
- 988 [40] Cheung JT-M, Zhang M. Parametric design of pressure-relieving foot orthosis using
989 statistics-based finite element method. Med Eng Phys 2008;30:269–77.
- 990 [41] Liu X, Zhang M. Redistribution of knee stress using laterally wedged insole
991 intervention: Finite element analysis of knee-ankle-foot complex. Clin Biomech
992 (Bristol, Avon) 2013;28:61–7.
- 993 [42] Tao K, Ji WT, Wang DM, Wang CT, Wang X. Relative contributions of plantar fascia
994 and ligaments on the arch static stability: A finite element study. Biomed Tech
995 2010;55:265–71.
- 996 [43] Chen W, Tang F, Ju C. Stress distribution of the foot during mid-stance to push-off in
997 barefoot gait : a 3-D finite element analysis 2001;16:614–20.
- 998 [44] Cheung JT-M, Zhang M, Leung AK-L, Fan Y-B. Three-dimensional finite element
999 analysis of the foot during standing--a material sensitivity study. J Biomech
1000 2005;38:1045–54.

- 1001 [45] Hsu Y-C, Gung Y-W, Shih S-L, Feng C-K, Wei S-H, Yu C-H, et al. Using an optimization
1002 approach to design an insole for lowering plantar fascia stress--a finite element study.
1003 *Ann Biomed Eng* 2008;36:1345–52.
- 1004 [46] Tao K, Wang D, Wang C, Wang X, Liu A, Nester CJ, et al. An In Vivo Experimental
1005 Validation of a Computational Model of Human Foot. *J Bionic Eng* 2009;6:387–97.
- 1006 [47] Mithraratne K, Ho H, Hunter PJ, Fernandez JW. Mechanics of Foot Part 2: A coupled
1007 solid-fluid model to investigate blood transport in the pathologic foot. *Int J Numer*
1008 *Method Biomed Eng* 2012;28:1071–81.
- 1009 [48] Guiotto A, Sawacha Z, Guarneri G, Avogaro A, Cobelli C. 3D finite element model of
1010 the diabetic neuropathic foot: A gait analysis driven approach. *J Biomech* 2014:1–8.
- 1011 [49] Sciumè G, Boso DP, Gray WG, Cobelli C, Schrefler BA. A two-phase model of plantar
1012 tissue : a step toward prediction of diabetic foot ulceration. *Numer Methods Biomed*
1013 *Eng* 2014.
- 1014 [50] Wang Y, Li Z, Zhang M. Biomechanical study of tarsometatarsal joint fusion using
1015 finite element analysis. *Med Eng Phys* 2014;36:1394–400.
- 1016 [51] Fontanella CG, Carniel EL, Forestiero A, Natali AN. Investigation of the mechanical
1017 behaviour of the foot skin. *Ski Res Technol* 2014:1–8.
- 1018 [52] Wong DW, Zhang M, Yu J, Leung AK. An investigation on joint force during walking
1019 using finite element analysis. *Med Eng Phys* 2014;36:1388–93.
- 1020 [53] NIU W, Tang T, Zhang M, Jiang C, FAN Y. An in vitro and finite element study of load
1021 redistribution in the midfoot. *Sci China Life Sci* 2014;57:1191–6.
- 1022 [54] Gefen a, Megido-Ravid M, Itzchak Y, Arcan M. Biomechanical analysis of the three-
1023 dimensional foot structure during gait: a basic tool for clinical applications. *J Biomech*
1024 *Eng* 2000;122:630–9.
- 1025 [55] Chen W, Lee S, Vee P, Lee S. Plantar pressure relief under the metatarsal heads –
1026 Therapeutic insole design using three-dimensional finite element model of the foot. *J*
1027 *Biomech* 2015;48:659–65.
- 1028 [56] Wang Y, Li Z, Wong DW, Zhang M. Effects of Ankle Arthrodesis on Biomechanical
1029 Performance of the Entire Foot. *PLoS One* 2015.
- 1030 [57] Guo J, Wang L, Mo Z. Biomechanical analysis of suture locations of the distal plantar
1031 fascia in partial foot. *Int Orthop* 2015.
- 1032 [58] Wang Z, Imai K, Kido M, Ikoma K, Hirai S. A Finite Element Model of Flatfoot (*Pes*
1033 *Planus*) for Improving Surgical Plan. *Conf Proc IEEE Eng Med Biol Soc*, vol. m, 2014, p.
1034 844–7.
- 1035 [59] Luboz V, Perrier A, Stavness I, Lloyd J, Bucki M, Cannard F, et al. Foot ulcer
1036 prevention using biomechanical modelling. *Comput Methods Biomech Biomed Engin*
1037 *2014*;2.
- 1038 [60] Perrier A, Bucki M, Luboz V, Vuillerme N, Payan Y. 3D musculoskeletal finite element
1039 analysis of the foot kinematics under muscle activation with and without ankle
1040 arthrodesis. *Comput Methods Biomech Biomed Engin* 2015;5842.
- 1041 [61] Perrier A, Luboz V, Bucki M, Vuillerme N, Payan Y. Conception and evaluation of a 3D

- 1042 musculoskeletal finite element foot model. *Comput Methods Biomech Biomed Engin*
1043 2015;18:2024–5.
- 1044 [62] Bandak FA, Tannous RE, Toridis T. On the development of an osseo-ligamentous
1045 finite element model of the human ankle joint. *Int J Solids Struct* 2001;38:1681–97.
- 1046 [63] Cheung JTM, Zhang M. Finite element and cadaveric simulations of the muscular
1047 dysfunction of weightbearing foot. *HKIE Trans Hong Kong Inst Eng* 2006;13:8–14.
- 1048 [64] Cho J-R, Park S-B, Ryu S-H, Kim S-H, Lee S-B. Landing impact analysis of sports shoes
1049 using 3-D coupled foot-shoe finite element model. *J Mech Sci Technol* 2009;23:2583–
1050 91.
- 1051 [65] Ji W-T, Tao K, Wang D-M, Wang C-T, Wang X. Mechanical behaviors of the foot after
1052 individual releases of plantar fascia and ligaments during the balanced standing. *J*
1053 *Shanghai Jiaotong Univ* 2010;15:726–9.
- 1054 [66] Luximon Y, Luximon A, Yu J, Zhang M. Biomechanical evaluation of heel elevation on
1055 load transfer - Experimental measurement and finite element analysis. *Acta Mech Sin*
1056 *Xuebao* 2012;28:232–40.
- 1057 [67] Bubanja D, Djukic A, Jurisic-Skevin A, Grbovic V, Saveljic I, Exarchos T, et al. Static and
1058 dynamic measurement and computer simulation of diabetic mellitus foot
1059 biomechanics. *J Serbian Soc Comput Mech* 2014;8:64–74.
- 1060 [68] Lin S-C, Chen CP-C, Tang SF-T, Chen C-W, Wang J-J, Hsu C-C, et al. Stress distribution
1061 within the plantar aponeurosis during walking - A dynamic finite element analysis. *J*
1062 *Mech Med Biol* 2014;14.
- 1063 [69] Forestiero A, Raumer A, Carniel EL, Natali AN. Investigation of the interaction
1064 phenomena between foot and insole by means of a numerical approach. *Proc Inst*
1065 *Mech Eng Part P J Sport Eng Technol* 2015;229:3–9.
- 1066 [70] Spears IR, Miller-Young JE, Waters M, Rome K. The effect of loading conditions on
1067 stress in the barefooted heel pad. *Med Sci Sports Exerc* 2005;37:1030–6.
- 1068 [71] Sopher R, Nixon J, McGinnis E, Gefen A. The influence of foot posture, support
1069 stiffness, heel pad loading and tissue mechanical properties on biomechanical factors
1070 associated with a risk of heel ulceration. *J Mech Behav Biomed Mater* 2011;4:572–82.
- 1071 [72] Chokhandre S, Halloran JP, van den Bogert AJ, Erdemir A. A three-dimensional
1072 inverse finite element analysis of the heel pad. *J Biomech Eng* 2012;134:31002.
- 1073 [73] Petre M, Erdemir A, Panoskaltsis VP, Spirka TA, Cavanagh PR. Optimization of
1074 Nonlinear Hyperelastic Coefficients for Foot Tissues Using a Magnetic Resonance
1075 Imaging Deformation Experiment. *J Biomech Eng* 2013;135.
- 1076 [74] Fontanella CG, Nalesso F, Carniel EL, Natali AN. Biomechanical behavior of plantar fat
1077 pad in healthy and degenerative foot conditions. *Med Biol Eng Comput* 2015.
- 1078 [75] Fontanella CG, Forestiero a, Carniel EL, Natali a N. Analysis of heel pad tissues
1079 mechanics at the heel strike in bare and shod conditions. *Med Eng Phys* 2013;35:441–
1080 7.
- 1081 [76] Fontanella CG, Favaretto E, Carniel EL, Natali AN. Constitutive formulation and
1082 numerical analysis of the biomechanical behaviour of forefoot plantar soft tissue. *J*

- 1083 Eng Med 2015;228:942–51.
- 1084 [77] Gu Y, Li J, Ren X, Lake MJ, Zeng Y. Heel skin stiffness effect on the hind foot
1085 biomechanics during heel strike. *Ski Res Technol* 2010;16:291–6.
- 1086 [78] Halloran J, Erdemir A, van den Bogert A. Adaptive Surrogate Modeling for Efficient
1087 Coupling of Musculoskeletal Control and Tissue Deformation Models. *J Biomech Eng*
1088 2009;131.
- 1089 [79] Nakamura S, Crowninshield RD, Cooper RR. An analysis of soft tissue loading in the
1090 foot--a preliminary report. *Bull Prosthet Res* 1981;10–35:27–34.
- 1091 [80] Halloran JP, Ackermann M, Erdemir A, van den Bogert AJ. Concurrent
1092 musculoskeletal dynamics and finite element analysis predicts altered gait patterns to
1093 reduce foot tissue loading. *J Biomech* 2010;43:2810–5.
- 1094 [81] Actis RL, Ventura LB, Lott DJ, Smith KE, Commean PK, Hastings MK, et al. Multi-plug
1095 insole design to reduce peak plantar pressure on the diabetic foot during walking.
1096 *Med Biol Eng Comput* 2008;46:363–71.
- 1097 [82] Lemmon D, Shiang TY, Hashmi a, Ulbrecht JS, Cavanagh PR. The effect of insoles in
1098 therapeutic footwear--a finite element approach. *J Biomech* 1997;30:615–20.
- 1099 [83] Spears IR, Miller-Young JE, Sharma J, Ker RF, Smith FW. The potential influence of the
1100 heel counter on internal stress during static standing: a combined finite element and
1101 positional MRI investigation. *J Biomech* 2007;40:2774–80.
- 1102 [84] Gefen A. Plantar soft tissue loading under the medial metatarsals in the standing
1103 diabetic foot. *Med Eng Phys* 2003;25:491–9.
- 1104 [85] Chen W, Lee PV. Explicit finite element modelling of heel pad mechanics in running :
1105 inclusion of body dynamics and application of physiological impact loads and
1106 application of physiological impact loads. *Comput Methods Biomech Biomed Engin*
1107 2015;5842.
- 1108 [86] Gefen a. Biomechanical analysis of fatigue-related foot injury mechanisms in
1109 athletes and recruits during intensive marching. *Med Biol Eng Comput* 2002;40:302–
1110 10.
- 1111 [87] Gefen a, Seliktar R. Comparison of the trabecular architecture and the isostatic
1112 stress flow in the human calcaneus. *Med Eng Phys* 2004;26:119–29.
- 1113 [88] Gefen A. Stress analysis of the standing foot following surgical plantar fascia release.
1114 *J Biomech* 2002;35:629–37.
- 1115 [89] Chatzistergos PE, Naemi R, Chockalingam N. A method for subject-specific modelling
1116 and optimisation of the cushioning properties of insole materials used in diabetic
1117 footwear. *Med Eng Phys* 2015;37:531–8.
- 1118 [90] Frahm KS, Mørch CD, Grill WM, Lubock NB, Hennings K, Andersen OK. Activation of
1119 peripheral nerve fibers by electrical stimulation in the sole of the foot. *BMC Neurosci*
1120 2013;14:116.
- 1121 [91] Frahm KS, Mørch CD, Grill WM, Andersen OK. Experimental and model-based
1122 analysis of differences in perception of cutaneous electrical stimulation across the
1123 sole of the foot. *Med Biol Eng Comput* 2013;51:999–1009.

- 1124 [92] Tadeipalli SC, Erdemir A, Cavanagh PR. Comparison of hexahedral and tetrahedral
1125 elements in finite element analysis of the foot and footwear. *J Biomech*
1126 2011;44:2337–43.
- 1127 [93] Yarnitzky G, Yizhar Z, Gefen a. Real-time subject-specific monitoring of internal
1128 deformations and stresses in the soft tissues of the foot: A new approach in gait
1129 analysis. *J Biomech* 2006;39:2673–89.
- 1130 [94] Luo G, Houston VL, Garbarini MA, Beattie AC, Thongpop C. Finite element analysis of
1131 heel pad with insoles. *J Biomech* 2011;44:1559–65.
- 1132 [95] Even-Tzur N, Weisz E, Hirsch-Falk Y, Gefen A. Role of EVA viscoelastic properties in
1133 the protective performance of a sport shoe: computational studies. *Biomed Mater*
1134 *Eng* 2006;16:289–99.
- 1135 [96] Verdejo R, Mills NJ. Heel-shoe interactions and the durability of EVA foam running-
1136 shoe midsoles. *J Biomech* 2004;37:1379–86.
- 1137 [97] Chen W, Lee S, Vee P, Lee S. The in vivo plantar soft tissue mechanical property
1138 under the metatarsal head : implications of tissues ' joint-angle dependent response
1139 in foot fi nite element modeling. *J Mech Behav Biomed Mater* 2014;40:264–74.
- 1140 [98] Spirka T a., Erdemir A, Ewers Spaulding S, Yamane A, Telfer S, Cavanagh PR. Simple
1141 finite element models for use in the design of therapeutic footwear. *J Biomech* 2014.
- 1142 [99] Khani MM, Katoozian H, Azma K, Naseh I, Salimi AH. Hyper-elastic parameter
1143 estimation of human heel-pad: A finite element and evolutionary based algorithm. *J*
1144 *Mech Med Biol* 2012;12.
- 1145 [100] Camacho D, Ledoux W, Rohr E, Sangeorzan B, Ching R. A three-dimensional,
1146 anatomically detailed foot model: a foundation for a finite element simulation and
1147 means of quantifying foot-bone position. *J Rehabil Res Dev* 2002;39:401–10.
- 1148 [101] <http://www.privatehealth.co.uk> 2015.
- 1149 [102] Chatzistergos PE, Naemi R, Chockalingam N. An MRI compatible loading device for
1150 the reconstruction of clinically relevant plantar pressure distributions and loading
1151 scenarios of the forefoot. *Med Eng Phys* 2014;36:1205–11.
- 1152 [103] V.J.Thomas, K.M.Patil SR. Three-dimensional stress analysis for the mechanics of
1153 plantar ulcers in diabetic neuropathy. *Med Biol Eng Comput* 2004;42:230–5.
- 1154 [104] Jacob S, Patil KM, Braak LH, Huson A. Stresses in a 3D two arch model of a normal
1155 human foot. *Mech Res Commun* 1996;23:387–93.
- 1156 [105] Noble P, Collin B, Lecomte-Beckers J, Magnée A, Denoix J, Serteyn D. An equine joint
1157 friction test model using a cartilage-on-cartilage arrangement. *Vet J* 2010;183:148–
1158 52.
- 1159 [106] Zhao Y, Zhang S, Sun T, Wang D, Lian W, Tan J, et al. Mechanical comparison between
1160 lengthened and short sacroiliac screws in sacral fracture fixation: A finite element
1161 analysis. *Orthop Traumatol Surg Res* 2013;99:601–6.
- 1162 [107] Chen WP, Tang FT, Ju CW. Stress distribution of the foot during midstance to push off
1163 in barefoot gait: a 3D finite element analysis. *Clin Biomech* 2001;16:614–20.
- 1164 [108] Dai XQ, Li Y, Zhang M, Cheung JTM. Effect of sock on biomechanical responses of foot

- 1165 during walking. Clin Biomech 2006;21:314–21.
- 1166 [109] Tao K, Ji W-TT, Wang D-MM, Wang C-TT, Wang X. Relative contributions of plantar
1167 fascia and ligaments on the arch static stability: A finite element study. Biomed Tech
1168 2010;55:265–71.
- 1169 [110] Petre MT. INVESTIGATING THE INTERNAL STRESS / STRAIN STATE OF THE FOOT
1170 USING MAGNETIC RESONANCE IMAGING AND We hereby approve the dissertation of.
1171 Case Western Reserve University, 2007.
- 1172 [111] Isvilanonda V, Iaquinto JM, Pai S, Mackenzie-helnwein P, Ledoux WR. Hyperelastic
1173 compressive mechanical properties of the subcalcaneal soft tissue : An inverse fi nite
1174 element analysis. J Biomech 2016;49:1186–91.
- 1175 [112] Spears IR, Miller-Young JE. The effect of heel-pad thickness and loading protocol on
1176 measured heel-pad stiffness and a standardized protocol for inter-subject
1177 comparability. Clin Biomech (Bristol, Avon) 2006;21:204–12.
- 1178 [113] Natali, Fontanella CG, Carniel EL. Constitutive formulation and analysis of heel pad
1179 tissues mechanics. Med Eng Phys 2010;32:516–22.
- 1180 [114] Hayes WC, Keer LM, Herrmann G, Mockros LF. A mathematical analysis for
1181 indentation tests of articular cartilage. J Biomech 1972;5:541–51.
- 1182 [115] Miller K, Lu J. On the prospect of patient-specific biomechanics without patient-
1183 specific properties of tissues. J Mech Behav Biomed Mater 2013;27:154–66.
- 1184 [116] Simkin A. Structural analysis of the human foot in standing posture. Tel Aviv
1185 University, Tel Aviv, Israel, 1982.
- 1186 [117] Halloran JP, Erdemir A. Adaptive Surrogate Modeling for Expedited Estimation of
1187 Nonlinear Tissue Properties Through Inverse Finite Element Analysis. Ann Biomed Eng
1188 2011;39:2388–2397.
- 1189 [118] Chatzistergos P, Naemi R, Chockalingam N. An MRI compatible loading device for the
1190 reconstruction of clinically relevant plantar pressure distributions and loading
1191 scenarios of the forefoot. Med Eng Phys 2014;36:1205–11.

1192
1193

1194 **Supplementary material caption:**

1195

1196 S1 Table: The database of studies that met the inclusion criteria and were included in
1197 this review. Detailed information about the methods used for model design,
1198 material assignment, loading and validation is presented. The studies are
1199 presented in alphabetical order based to the surname of the first author.